



# Geotechnical and chemical characterization of expansive clayey soil amended by biochar derived from invasive weed species *Prosopis juliflora*

Anasua GuhaRay<sup>1</sup> · Mei Guoxiong<sup>2</sup> · Arijit Sarkar<sup>1</sup> · Sanandam Bordoloi<sup>3</sup> · Ankit Garg<sup>3</sup> · Spandan Pattanayak<sup>1</sup>

Received: 30 May 2019 / Accepted: 10 September 2019 / Published online: 17 September 2019  
© Springer Nature Switzerland AG 2019

## Abstract

Biochar is biomass-derived carbonaceous solid product obtained when plant-based biomass is heated in a closed environment in presence of little or no oxygen. In the present study, the biochar is produced by slow pyrolysis of *Prosopis Juliflora*. The use of *P. Juliflora* helps to reduce the threat to biodiversity as well as decrease the transmission rate of malaria, thus contributing to a sustainable environment. The biochar is uniformly mixed with expansive black cotton soil at three different percentages (5, 10% w/w) at same compaction state. Microstructural (X-ray diffraction, Fourier-transform infrared spectroscopy, scanning electron microscope, energy-dispersive x-ray spectroscopy), physicochemical (cation exchange capacity, pH, specific gravity) as well as geotechnical characterizations (consistency limits, free swell, permeability, California bearing ratio (CBR), shear strength) are carried out on soil with and without biochar amendment at different percentage mix by laboratory testing. It is observed that addition of biochar increases the shear strength and CBR and decreases the free swell index of the expansive soil. Overall, the study revealed that biochar-amended soils can possess excellent geotechnical properties to serve as a stabilizing material for expansive soils.

**Keywords** Expansive clay · Biochar amendment · Chemical analysis · Geotechnical characterization

## Introduction

*Prosopis juliflora* is regarded as invasive in many countries such as Asia, Australia and Africa [1, 2] and Hawaii, USA [3]. It has created a negative biodiversity in many parts of the world [2]. It is known to grow rapidly due to its inbuilt mechanism or characteristics to overcome drought and salinity stress. This is enhanced by its high ‘proline’ content under these stress conditions. The invasive species can withdraw water from deeper layers due to its deep penetrating roots.

In addition to the threat to biodiversity, the *Prosopis juliflora* species also contributes immensely in enhancing the transmission capacity of disease called “malaria” [4]. Field experiments were carried out to investigate *Anopheles gambiae* populations in villages with and without the presence of *Prosopis juliflora* [4]. It was found from the study that the *Anopheles gambiae* population can almost be doubled due to presence of *Prosopis juliflora*. The reason is that this invasive plant is an important source of sugar for older and larger mosquito population especially during the dry season.

---

✉ Anasua GuhaRay  
anasua08@gmail.com

✉ Mei Guoxiong  
meiguox@163.com

Arijit Sarkar  
arijits340@gmail.com

Sanandam Bordoloi  
sanandambordoloiaec95@gmail.com

Ankit Garg  
ankit@stu.edu.cn

Spandan Pattanayak  
f20160489@hyderabad.bits-pilani.ac.in

<sup>1</sup> Department of Civil Engineering, BITS-Pilani Hyderabad, Secunderabad 500078, India

<sup>2</sup> College of Civil Engineering and Architecture, Guangxi University, Nanning, China

<sup>3</sup> Department of Civil and Environmental Engineering, Shantou University, Shantou, China

This would therefore help in extending the survival rate of mosquitos and hence, the transmission season of malaria.

Though, there are various control strategies such as by conversion to flour production or charcoal production for agricultural yield [5] that has been explored, but its conversion to biochar (BC) for utility as cover material (i.e., when mixed with soil) in green infrastructures (green roof, biofilter units; vegetated slopes) is relatively less explored. Some recent studies were done by the agriculturalists to analyze use of BC produced from *Prosopis Juliflora* in soil fertility and agricultural crops yield [6, 7]. Their studies found out that BC from *Prosopis juliflora* increases plant productivity and is also able to adsorb chromium contaminant. The effects of biochar (5%, 10% and 15% by weight) amendment on physicochemical and geotechnical properties of landfill cover soil showed that the hydraulic conductivity of the soil increases, compressibility of the soil decreases and shear strength of the soil increases with an increase in the biochar amendment and with a decrease in biochar particle size [8]. The engineering properties of seven different types of waste wood-derived biochar and biochar-amended soils were studied for engineering applications [9]. It was observed that biochar amendment to soil increases the porosity, water holding capacity and organic matter and decreases the density and specific gravity of soil. The physical and chemical properties of commercially available waste wood-derived biochar fixed carbon, volatile matters and ash content vary with the type of production [10]. The effects of biochar on shear strength and liquefaction properties of cohesionless soils showed that biochar-amended soil delays the increase in excess pore water pressure and provides some resistance to liquefaction [11]. The rate of soil erodibility of biochar-amended soil, to be used as a cover material for geo-environmental applications, decreased with gradual increment in water content [12]. The water retention and gas permeability characteristics of biochar-amended soil and its relationship with soil water content in unsaturated state were also investigated [13]. The microstructural and morphological characterization of lead contaminated clay with zero-valent iron treatment exhibited larger particle size and branched particle shape [14]. A new model based on model uncertainty characterization was proposed for estimating root cohesion of Riparian trees [15]. Treating lead contaminated soil with zero-valent iron caused an increase in the vane shear strength, stiffness, friction angle and compression index of the soil [16]. The feasibility of nanoscale zero-valent iron (nZVI) for simultaneous stabilization of Pb and improvement of soil strength is demonstrated via batch experiments [17]. A correlation is derived between the unsaturated shear strength parameters of silty sand and its unconfined compressive strength [18].

However, limited studies reported that analyze index and engineering properties of soil mixed with biochar are produced from *Prosopis Juliflora*. Further, the soil density

adopted in green infrastructure (i.e., slopes) is relatively higher (i.e., 95% degree of compaction) as compared to that in agricultural fields (i.e., 50–60% degree of compaction) [10, 19]. Difference in packing of soil particles may influence the soil pores size and arrangement. This may further affect how fine biochar interacts with the soil pores. Therefore, it is important to understand the influence of biochar on the compacted soil properties (i.e., index as well as mechanical) often found in green infrastructures. Further, there are relatively less studies that analyze changes in physio-chemical characterization (using SEM, XRD, FTIR, etc.) of compacted soil when mixed with BC produced from *P. Juliflora*. Such characterization is important to understand the interaction of compacted soil and biochar and further interpret engineering properties of soil. This may help to explore feasibility of such BC produced from invasive and malaria contributing plant in green infrastructures. This might lead to an alternate means of waste management for this invasive plant. In addition to this, BC can facilitate the stability of the carbon in green infrastructure and help in long-term carbon sequestration [20].

The main objective of the present study is to investigate the index and engineering properties of an expansive soil amended with *Prosopis Juliflora* BC. The BC is produced by slow pyrolysis of local *Prosopis Juliflora* and uniformly mixed with soil at three different percentages (0, 5 and 10) at same compaction state. The biochar from a specific weed promotes malaria. The usage of such weed for biochar production will help to keep malaria in check. Physio-chemical characterization is carried out on soil with and without biochar at different percentage mix. Their mineralogical, microstructural, physical and chemical characteristics are compared to assess their potential for the purpose of ground improvement.

## Materials used

### Black cotton soil

In the present study, the expansive black cotton soil (BCS) is collected from Nalgonda district of Telangana state in the southern part of India. The soil is classified as highly compressible clay (CH) according to Unified Soil Classification System. The different physicochemical, index and engineering properties of BCS are provided in Table 1. The tests are conducted according to ASTM 4318-93, ASTM D1557 and ASTM D2166-98 (ASTM 2000c; ASTM 2012).

### Biochar

Biochar is produced from invasive *Prosopis juliflora*. The production of biochar is carried out using slow pyrolysis

**Table 1** Basic properties of black cotton soil

Properties	Values
Physicochemical properties	
pH	8.35
Cation exchange capacity (meq/100 gms)	
Calcium	4.832%
Sodium	0.780%
Potassium	2.832%
Magnesium	0.644%
Silica	42.67%
Aluminum	13.82%
Index and engineering properties	
Specific gravity	2.59
Liquid limit (LL)	62%
Plastic limit (PL)	20%
Plasticity index (PI)	42%
Shrinkage limit (SL)	12%
Grain size distribution	
Gravel (> 4.75 mm)	1%
Sand (0.075–4.75 mm)	27%
Silt and Clay (< 0.075 mm)	72%
Soil classification (according to USCS)	CH
Free swell index (FSI)	76.3%
Maximum dry density (MDD)	16.5 kN/m <sup>3</sup>
Optimum moisture content (OMC)	17.6%
Permeability (cm/sec)	$7.2 \times 10^{-7}$
Soaked California bearing ratio (CBR)	1.92
Unconfined compressive strength	185 kN/m <sup>2</sup>

process [21, 22] in a muffle furnace. The temperature for pyrolysis is kept at around 500 °C. The biochar contains particles ranging around size equivalent to 55% medium sand, 40% dense sand and 5% of total fines (silt and clay) fraction. Based on the elemental analysis [23], the biochar contains around 75% carbon (C) and 0.25% nitrogen (N) content. The C/N ratio is found to be around 395, whereas CEC of biochar is 21 cmol/kg.

## Experimental methodology

### Chemical characterization

X-ray diffraction (XRD) analyses are performed using a RIGAKU Ultima IV diffractometer to identify the minerals present in the untreated and treated BCS. The powdered samples are examined through CuK $\alpha$  rays generated at 40 mA and 40 kV. The operating  $2\theta$  range is from 0 to 100° with a step of 0.02° for  $2\theta$  values and integrated at the rate of 2 s per step. Fourier-transform infrared (FTIR) spectroscopy of BCS is collected using a JASCO FTIR 4200 setup.

The BCS is powdered and dried in an oven at 105 °C for 1 h to remove any residual moisture and then mixed with dried KBr powder to prepare pellets. The spectral range is specified as 4000–400 cm<sup>-1</sup> for all the samples. The FTIR spectra for BCS are performed to study the change in the formation of chemical bonds following the treatment by analyzing the transmittance spectra. The SEM–EDS study is conducted using Thermo Scientific Apreo SEM provided by FEI (Field Electron and Ion Company). The images of different magnification are captured, at various locations of BCS. At each location, three different regions are chosen at random for detecting the surface topography at 1250 and 2500 magnifications. The EDS spectra are also provided through software system which measures the relative abundance of emitted X-rays along with their energy. For the adequate working of EDS analyzer, the probe current and working distance are maintained at 65.4 ~ 67.0  $\mu$ A and 8–15 mm. Micrographs are randomly chosen for detecting the surface topography at 2500  $\times$ , 5000  $\times$  and 10000  $\times$  magnifications at three different locations. At each location two images are captured at different ranges.

### Geotechnical characterization

To test the Atterberg limits (LL, PL and PI), the BC blended black cotton soil is pulverized and tested as per ASTM D 4318 (ASTM 2000a). A series of standard Proctor compaction tests are conducted on black cotton soil incorporated with 0, 5 and 10% of BC in order to achieve the density–moisture relationship of soil stabilizer. The undrained shear strength test of cohesive soil is performed according to ASTM D2166 standard. Multiple unconfined compressive strength (UCS) tests for all composite soil are conducted in the laboratory under a fixed strain rate of 1.2 mm/min in order to assess the increasing amount of shear strength behavior with addition of BC. Before preparing the sample, the OMC of the particular soil is evaluated through Proctor compaction test at varying percentages of BC. Treated and untreated soils are molded in 3.8 cm diameter by maintaining the height as twice the diameter by mixing the particular OMC in the soil with respect to that curing period. After sample preparation, it is kept in an airtight vacuum desiccator for maturation and to preserve the moisture content during compressive load application. Free swell index is one of the simplest tests used to identify the expansiveness and swelling potential of soil by adopting the ASTM D2166-06 procedure. This test is performed by transferring 10 g of BC blended soil passing through IS 4.75 mm sieve in two graduated cylinders of 100 cc volume filled with distilled water and kerosene. After 24 h, the volume of soil is measured against the graduated jar and found the differential swelling percentage. Soaked CBR test is conducted for both untreated and BC-treated expansive soil through

ASTM D1883—16 to evaluate the suitable stiffness of a subgrade layer by soaking the soil samples for 96 h in water prior to the test. Static load at the rate of 1.25 mm/min was applied on the specimen through a loading frame of 50 mm dia. plunger. Observations are taken between the test load (penetration resistance) versus the penetration of plunger at 2.5 and 5 mm, respectively.

## Results and discussions

### Chemical characterization

#### X-ray diffraction (XRD)

X-ray diffraction peaks obtained for powdered samples of untreated BCS as well as AAB-treated BCS are shown in Fig. 1a–d. XRD analysis shows that the raw BCS consisted of clay minerals such as montmorillonite (M), quartz (Q) illite (I) and muscovite (Ms) (Fig. 1). This is consistent with the findings of previous researchers [24–27].

From Fig. 1, it can be observed that for pure biochar, the peak at around  $20^{\circ}$ – $22^{\circ}$  can be attributed to the mineral apatite (Ap). The broad peak at  $26^{\circ}$  is indicative of the presence of the amorphous carbon in the sample, due to formation of turbostratic carbon crystallites. The peaks at around  $40^{\circ}$  are due to the mineral calcite (C) which is a common mineral in the biochar. The peaks at around  $30^{\circ}$  represent quartz (Q) and anhydrite (A) (at  $29^{\circ}$ ).

The peak in the graph suggests that at  $2\theta$ , the structure is more crystalline in nature. It can be observed from Fig. 1 that as 5% biochar is mixed in the black cotton soil, the intensity of the peaks increased because of the attribution

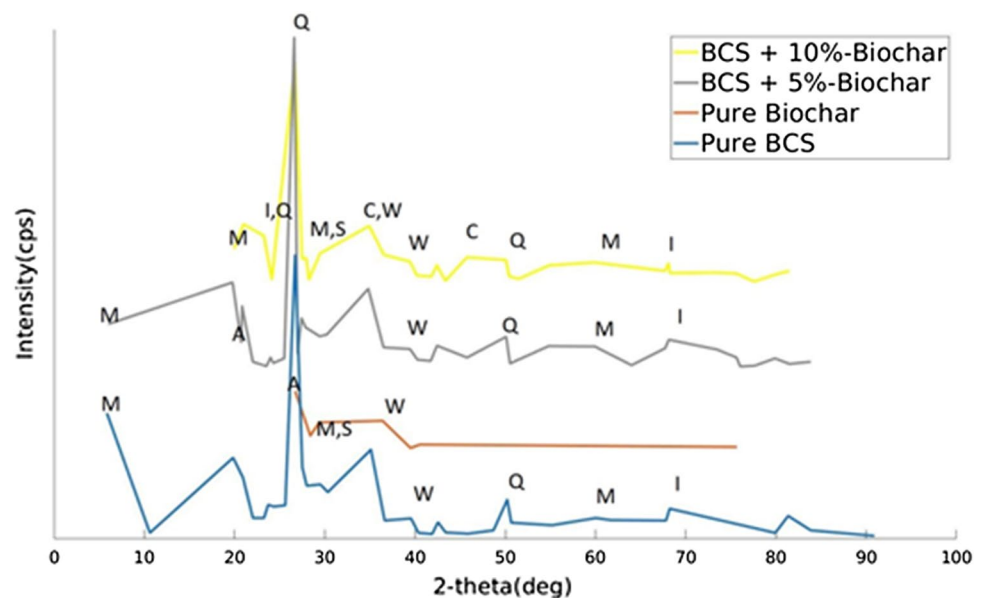
of crystallinity by hemicellulose and lignin present in biochar, hence sharper peak is obtained. As 10% biochar by weight is mixed with soil, the inter-planar spacing between the soil particles is increased and peaks of low intensity are obtained. As black cotton soil is clayey in nature, so it consists the clayey minerals such as montmorillonite (M), quartz (Q), illite (I) and muscovite (Ms) which can also be seen from the peaks of graphs that correspond to these minerals. Because of biochar present in soil, the graphs also show some peaks for the minerals that corresponds to sylvite (S), calcite (C), whitlockite (W). In 5% biochar-BCS mix, the peaks of smaller intensity are obtained that corresponds to sylvite mineral, but in 10% biochar-BCS mix, these peaks are absent for this mineral. Due to more addition of biochar, the inter-planar spacing between the soil particles increases and the structure loses its crystallinity.

#### Fourier-transform infrared (FTIR) spectroscopy

FTIR spectroscopy compares the presence of different chemical bonds and molecular vibrations in untreated and BC-treated black cotton soil. The corresponding transmittance spectra are presented in Fig. 2. From the figure, it is observed that untreated BCS shows peaks at  $2924\text{ cm}^{-1}$  for C–H (asymmetric stretching), C–H stretching at  $2855$  similarly at  $2350$  for C=O (symmetric),  $1633$  for C=O (stretching),  $1439$  for C–H (bending),  $1033$  for Si–O–Si (antisymmetric stretch), for Al–O (stretching) at  $785$  and at  $527$  for Si–O–Al (bending) vibrations [26, 27].

In Fig. 2, the peaks for the pure biochar are observed at the frequencies— $3739.3$ ,  $3428.8$ ,  $2921.6$ ,  $2856.1$ ,  $2169.5$ ,  $1897.6$ ,  $1583.3$ ,  $1444.4$ ,  $1147.4$ ,  $1004.7$ ,  $876.5$ ,  $753.1$  and  $515.9\text{ cm}^{-1}$ . Vibration of silanol group at hetero-boundary

**Fig. 1** X-ray diffractogram of raw BCS, pure biochar and BCS amended with 5% and 10% biochar



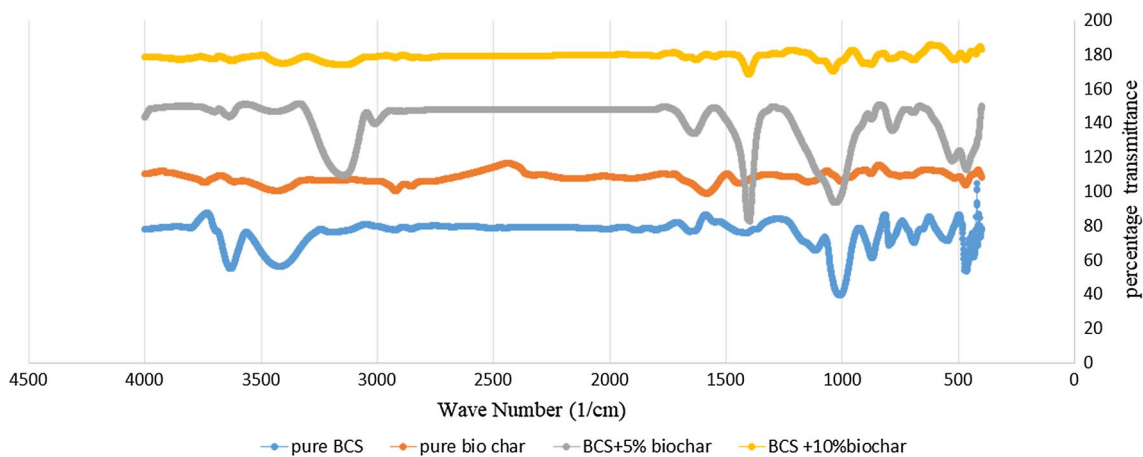


**Fig. 2** FTIR spectral image profile of raw BCS, pure biochar and soil amended with 5% and 10% biochar

is captured by the peak at  $3739.3\text{ cm}^{-1}$ ; similarly hydroxyl group's vibration is captured by the peak at  $3428.8\text{ cm}^{-1}$ .  $2921.6$  and  $2856.1\text{ cm}^{-1}$  represent the C–H vibration and the symmetric C–H bond, respectively. Combination of the amide I band with that of the amide III band is captured by the peak at  $2169.5\text{ cm}^{-1}$ . Presence of Rh–NO+ species is denoted by the peak at  $1897.6\text{ cm}^{-1}$ . Peak at  $1583.3\text{ cm}^{-1}$  corresponds to C–C stretching of benzene ring. Polymerization of Si–OH groups forming Si–O–Si bonds in inner structures is given by the peak at  $1147.4\text{ cm}^{-1}$ . The peaks at  $876.5$  and  $753.1\text{ cm}^{-1}$  represent the asymmetric bending of calcite and SiAOAl symmetric vibration, respectively. Stretching vibration of the bond between manganese and oxygen is shown by the peak at  $515.9\text{ cm}^{-1}$ . The peak at  $469.6\text{ cm}^{-1}$  represents the  $\text{CH}_2$  and  $\text{CH}_3$  deformation.

From Fig. 2, it is observed that untreated BCS + 5% biochar shows peaks at  $3636, 3436, 3147, 3010, 1639, 1398, 1031, 785$  and  $467\text{ cm}^{-1}$ . The bands at  $3636, 3436, 3147$  and  $1639\text{ cm}^{-1}$  indicate the presence of water and are associated with O–H stretching vibrations. The band at  $1398\text{ cm}^{-1}$  represents symmetric stretching of  $\text{COO}^-$  groups. The bands at  $1031$  and  $693\text{ cm}^{-1}$  are assigned to symmetric stretching of Si–O. The Si–O–Si bending is represented by peak at  $468\text{ cm}^{-1}$ . Figure 2d presents the FTIR spectra of BCS with 10% biochar. With increase in percentage of biochar, additional peaks were observed in the FTIR spectra. The major bands were at  $3840, 3408, 3144, 1403, 1039, 875$  and  $691\text{ cm}^{-1}$ . The bands at  $3840, 3616, 3408$  and  $1624\text{ cm}^{-1}$  are assigned to O–H stretching of water. The deformational vibrations of methyl groups are indicated by peak at  $1403\text{ cm}^{-1}$ . The Si–O stretching vibrations are associated with peaks at  $793$  and  $468\text{ cm}^{-1}$ .

With the increase in the biochar content, the number of peaks corresponds to different types of stretching and vibrations increased. This is because of the surface active groups like hydroxyl, amine, carboxyl, etc. of hemicelluloses, lignin

(polymers present in biochar) that are capable to bind with the heavy metals and increased the chemical bonding. The carboxyl, hydroxyl, amino groups are the hydrophilic groups which attract the water and increase the bonding and hence liquidity limit (LL) will increase. With the increase in percentage of biochar, there is an increase in the number of peaks in the FTIR spectra. The chemical shift observed in the spectra with an increase in percentage of biochar is presented in Table 2.

### Scanning electron microscopy (SEM)

Figure 3 shows the scanning electron micrographs for BCS treated with varying percentages of AAB Typical micrograph of raw BCS shows the clay layers in the figure which reveals a flaky type microstructure indicating smectite and montmorillonite surface layer of clay matrix [24].

The microstructures of biochar depend on wood species and post-processing on the raw material (Fig. 4). The magnified images of biochar show the honeycomb structure, and regular shape vessels are also visible. A structural deformation can occur or removal and also relocation of cell wall matrix (change in cell structure) due to the effect of a high temperature and microwave frequency. Bigger porous holes are visible. Porosity of biochar develops the soil in such a way that in dry conditions, biochar holds the moisture long

**Table 2** Chemical shift due to presence of different biochar contents

BCS + 5% biochar	BCS + 10% biochar
3142	3144 (–2)
1639	1625 (14)
1399	1403 (–11)
784	793 (–9)
525	516 (–9)

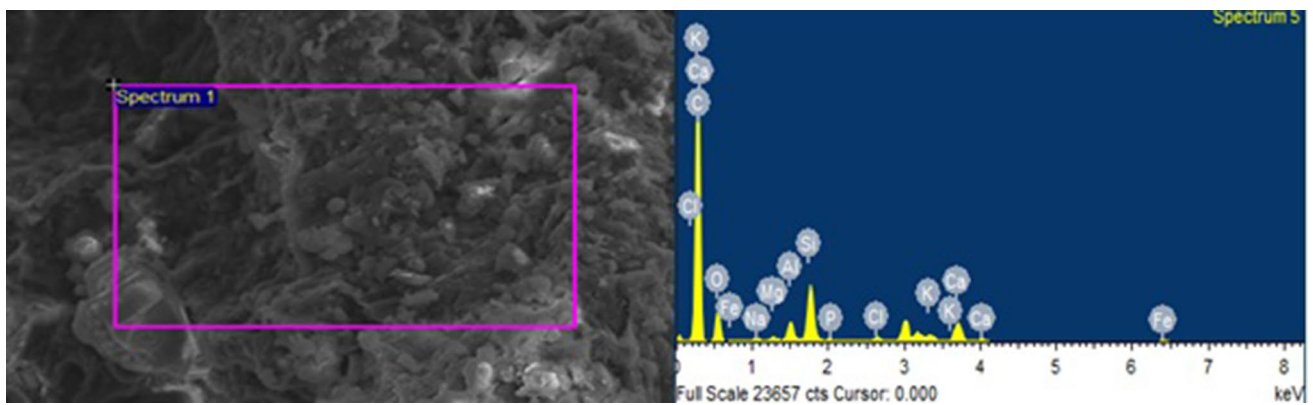


Fig. 3 SEM-EDS images of raw BCS

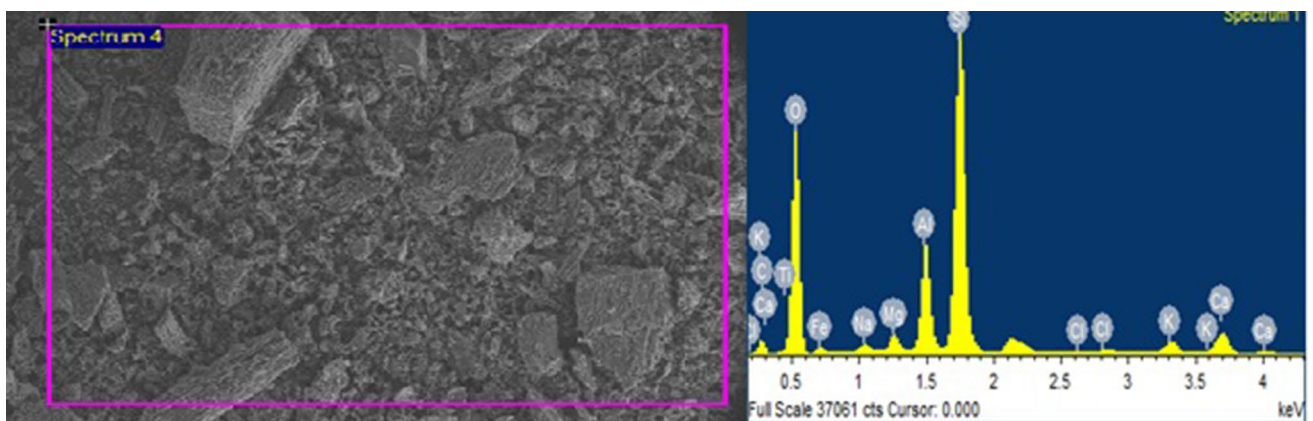


Fig. 4 SEM-EDS images of pure biochar

after the surrounding soil, and aids to facilitate the behavior of water and air in soil and allows microbial life to stay alive in periods of drought. In this way, biochar assists to boost the soil fertility. As the pyrolysis temperature of biochar increases, the maximum carbon content increases and the volatile matter decreases. Many white dots are found on the surface of biochar. These white dots comprise of silicon. It is also possible that crystallinity (more regular packing) of mineral components increases and highly ordered aromatic structures form with increasing pyrolysis temperature. The sphere-like microparticles are formed by the degradation of cellulose and lignin during carbonization.

Figure 5a, b shows the SEM images of black cotton soil mixed with 5% and 10% of biochar. From the figures, we can see flaky layers of black cotton soil accompanied with solid framework of biochar matrix. With increase in biochar, the cellular matrix density increases and in Fig. 5b, it is seen that the cellular matrix places itself in between the flaky layers, which can aid in improving the bearing capacity of soil. Additionally, the soil looks more porous than it was before biochar treatment.

EDS provides the chemical composition in weight percent (Wt%) and atomic percent (At%) for black cotton soil treated with different percentages of BC shown in Table 3. As expected, silica (Si) and calcium (Ca) are found to be the major components of the untreated BCS. Oxygen (O) and carbon (C) are also found along with traces amount of aluminum (Al) peaks in Fig. 5a.

### Geotechnical characterization

Table 4 provides the basic geotechnical characteristics of soil amended with 5% and 10% of biochar. The specific gravity of biochar is 0.85. The specific gravity of soil amended with 0, 5 and 10% of biochar are 2.59, 2.50 and 2.45, respectively. The reason for the lower specific gravity of soil amended with biochar may be attributed to the fact that the soil particles are replaced by organic biochar particles that have a lower dry density than soil particles.

The MDD and corresponding OMC for raw BCS are  $16.5 \text{ kN/m}^3$  and 17.6%, respectively. By adding biochar, MDD decreased while OMC increased. It may be stated that

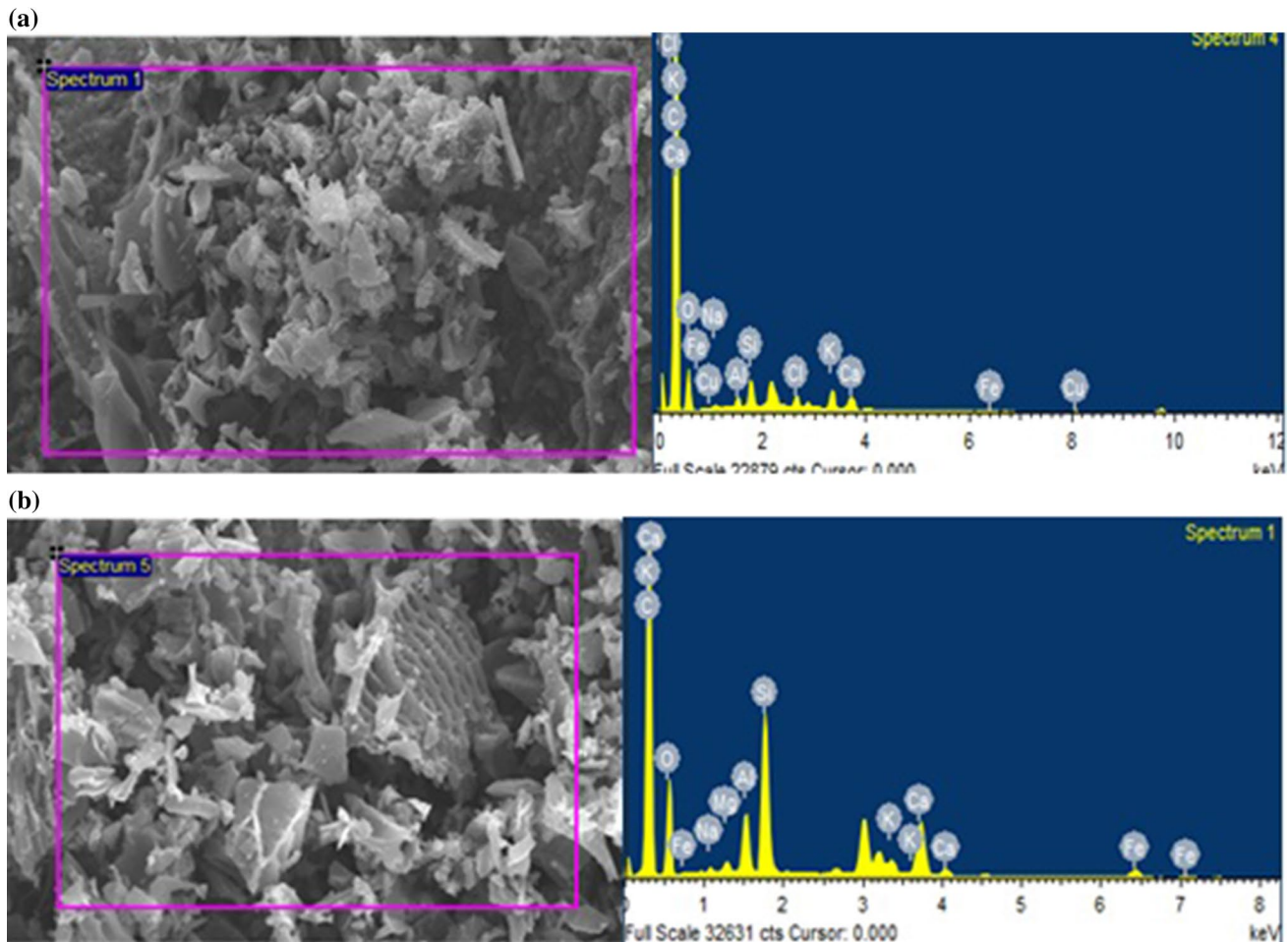


Fig. 5 SEM-EDS images (at 2500x magnification) of a soil + 5% biochar b soil + 10% biochar

Table 3 EDS elemental analysis for untreated BCS, biochar & biochar-amended soil

Elements/ Samples	Pure biochar		BCS + 5% biochar		BCS + 10% biochar		Untreated BCS	
	Weight (%)	Atomic (%)	Weight (%)	Atomic (%)	Weight (%)	Atomic (%)	Weight (%)	Atomic (%)
C	11.86	18.22	22.22	17.60	163.88	23.75	61.01	19.57
O	51.44	59.30	98.51	58.60	59.70	55.45	21.99	53.47
Na	0.62	0.50	0.70	0.29	16.73	12.85	40.73	6.83
Al	6.51	4.45	17.37	6.13	32.27	2.08	36.65	5.23
Si	20.88	13.71	33.95	11.50	82.89	5.14	91.08	12.50
Cl	0.15	0.08	0.00	0.00	0.00	0.00	0.00	0.00
K	1.06	0.50	2.00	0.49	2.22	0.10	4.47	0.44
Ca	2.19	1.01	19.66	4.67	9.33	0.41	8.20	0.79
Fe	3.90	1.29	0.00	0.00	0.00	0.00	9.96	0.69

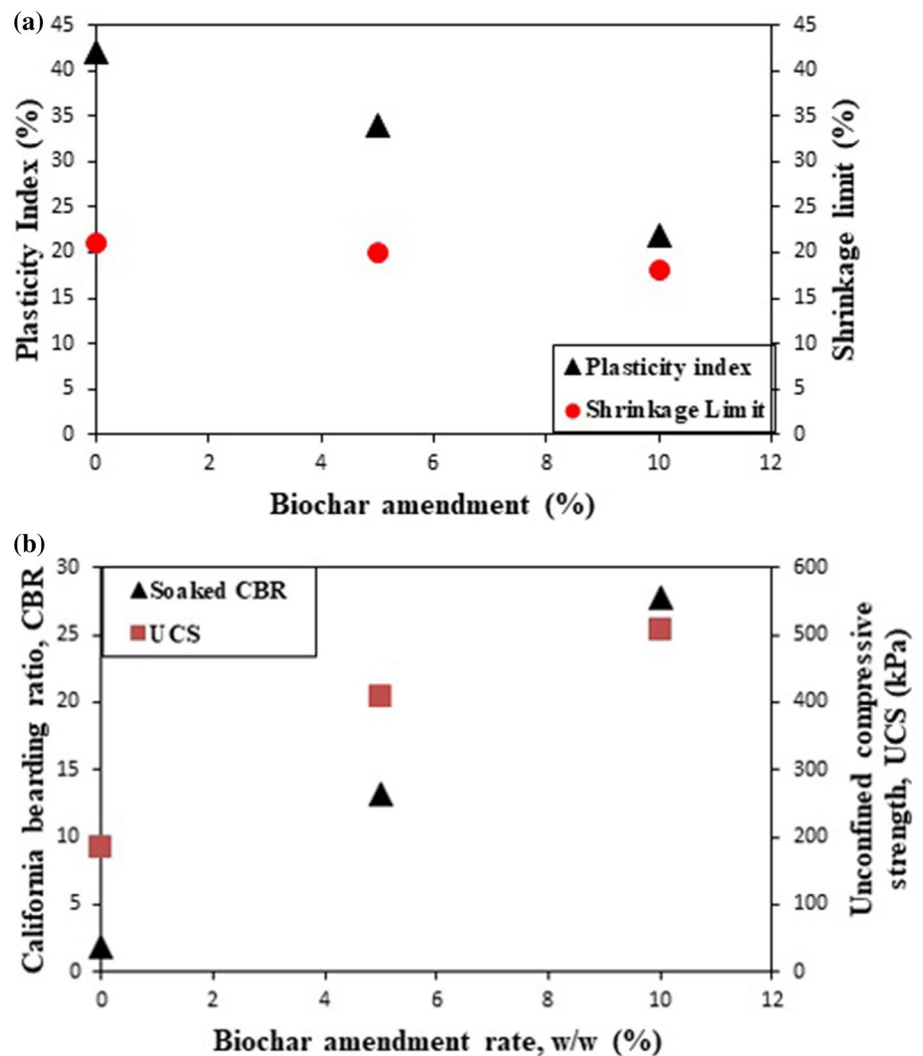
the decreased MDD is mainly due to the lower specific gravity of biochar particles [28] and the smaller compressibility of amended soils at a given compaction energy [29]. The higher OMC can be caused by the highly porous structure and larger surface area of biochar particles.

Figure 6a shows the variation of plasticity index and shrinkage limit in biochar-amended soil. The Atterberg limit test on biochar revealed it to be non-plastic. The decrease in plasticity index indicates that addition of biochar to black soil decreases its plasticity. It is attributed to more

**Table 4** Physio-chemical properties of black cotton soil amended with 5% and 10% of biochar

Properties	Pure biochar	5% Biochar	10% Biochar
Physicochemical properties			
pH	9.25	9.37	9.30
Index and engineering properties			
Specific gravity	0.85	2.50	2.45
Liquid limit (LL)	NP	49%	55%
Plastic limit (PL)	NP	15%	33%
Grain size distribution			
Gravel (> 4.75 mm)	0%	1%	1%
Sand (0.075–4.75 mm)	38%	27%	27%
Silt and clay (< 0.075 mm)	62%	72%	72%
Soil classification (according to USCS)			
Free swell index (FSI)	–	69.3%	60%
Permeability (cm/sec)	–	$5.9 \times 10^{-6}$	$7.7 \times 10^{-5}$
Maximum dry density (MDD) (kN/m <sup>3</sup> )	–	16.1	15.6
Optimum moisture content (OMC) (%)	–	18	18.5

**Fig. 6 a** Variation of plasticity index and shrinkage limit of BCS with biochar amendment. **b** Variation of soaked CBR and UCS of BCS with biochar amendment





cohesionless material entering the matrix in a soil having more clay particles. This is in contrast to biochar amendment in silty soil, wherein addition of biochar results increases in liquid and plastic limit [12]. There is no significant change in the shrinkage limit of the soil regardless of biochar percentage which is consistent to the findings of previous studies [12].

With respect to mechanical strength (Fig. 6), it is clearly observed that soaked CBR increases with gradual biochar addition (almost 2.6 times). The increase in strength by both UCS and CBR can be attributed to the hydrophilic surface functional groups (mainly hydroxyl) observed in the FTIR of biochar. Thus, surface cohesive bonds are magnified with biochar addition. Furthermore, as the soil is constituted of charged clay particles (indicated in Table 1), the negative ions can form bonds with the surface functional groups (indicated by change in absorbance through wavelength (1000–2000) for biochar-amended soil).

**Soil water characteristics curve (SWCC)**

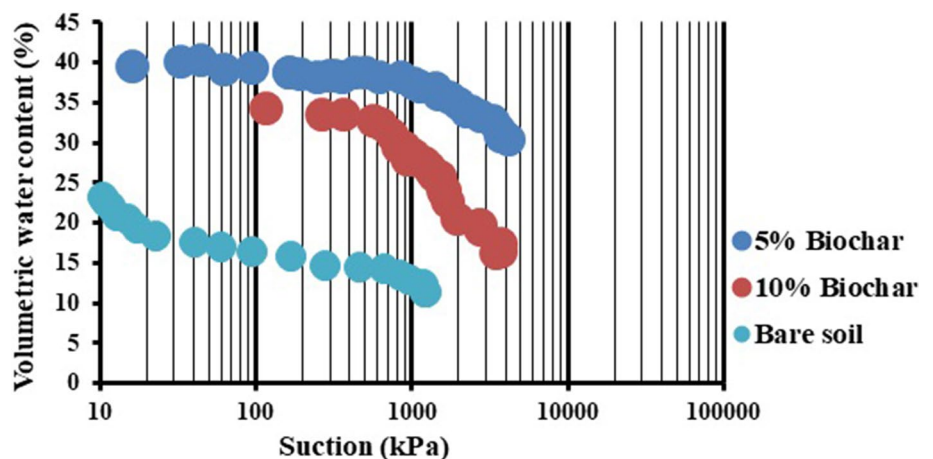
Figure 7 shows the soil water characteristic curves for raw BCS and BCS amended with 5% and 10% of biochar. It is seen from Fig. 7 that the water retention increases with addition of biochar. This increase can be attributed to the high amount of intrapores within the biochar. Secondly, the hydrophilic groups in the biochar surface further attract the water molecules. Based on the sensor readings, the air entry value potentially increases with addition of biochar as well. In previous studies [30–32], the biochar produced from water hyacinth also shows significant increase in water retention of silty sandy soil. The effect of biochar in case of sandy soil appears to be more prominent than that in the expansive soil (in current study). This might be due to relative difference in porous structure of biochar and the soil under investigation.

**Conclusion**

The present study investigates the index and engineering properties of expansive black cotton soil amended with *Prosopis Juliflora* biochar, uniformly mixed with soil at three different percentages (0, 5 and 10). The use of *P. Juliflora* serves a bifold purpose of reducing the threat to biodiversity as well as decreasing the transmission rate of malaria, thus contributing to a sustainable environment. The following conclusions can be derived from the present study:

- The plasticity index of the biochar-amended soil decreased by a considerable amount with increase in percentage of biochar addition. The free swell index of the soil also decreases with addition of biochar, which leads to the stabilization of expansive soil. However, there is no significant change in the shrinkage limit of the soil regardless of biochar percentage.
- MDD decreased while OMC increased with addition of biochar. The decreased MDD is mainly due to the lower specific gravity of biochar particles and the smaller compressibility of amended soils at a given compaction energy. The higher OMC can be caused by the highly porous structure and larger surface area of biochar particles.
- The CBR value increased by almost 2.6 times with addition of biochar. Also the unconfined compressive strength increased significantly with biochar amendment. The increase in strength by both UCS and CBR can be attributed to the hydrophilic surface functional groups (mainly hydroxyl) observed in the FTIR of biochar.
- The soil water characteristic curve shows that the water retention capacity of expansive soil increases with addition of biochar. This is due to the high amount of intrapores within the biochar and the hydrophilic groups present on the biochar surface.

**Fig. 7** Soil water characteristic curves for **a** soil, **b** soil + 5% biochar, **c** soil + 10% biochar



The limitation of current study is that only one type of soil and biochar has been used. In addition, testing has been done for a limited duration of time without considering any effects of degradation of biochar. A large-scale study considering soil–biochar mix with a long-term monitoring is required to capture degradation effects of biochar.

**Acknowledgements** The authors would like to express their sincere gratitude to the Central Analytical Laboratory Facilities at BITS-Pilani, Hyderabad Campus for providing the setup for the XRD, FTIR and SEM–EDS analyses.

## References

- Mwangi E, Swallow B (2005) Invasion of *Prosopis juliflora* and local livelihoods: case study from the lake Baringo area of Kenya. World Agroforestry Centre, Nairobi
- Gallaher T, Merlin M (2010) Biology and impacts of Pacific island invasive species. 6. *Prosopis pallida* and *Prosopis juliflora* (Algarroba, Mesquite, Kiawe) (Fabaceae). *Pac Sci* 64(4):489–526
- Pasiecznik NM, Felker P, Harris PJC, Harsh LN, Cruz G, Tewari JC, Cadoret K, Maldonado LJ (2001) The *Prosopis juliflora*—*Prosopis pallida* complex: a monograph. HDRA, Coventry, p 172
- Muller Gunter C, Junnila Amy, Traore Mohamad M, Traore Sekou F, Doumbia Seydou, Sissoko Fatoumata, Dembele Seydou M, Schlein Yosef, Arheart Kristopher L (2017) The invasive shrub *Prosopis juliflora* enhances the malaria parasite transmission capacity of *Anopheles* mosquitoes: a habitat manipulation experiment. *Malar J* 16:237. <https://doi.org/10.1186/s12936-017-1878-9>
- Wakie TT, Hoag D, Evangelista PH, Luizza M, Laituri M (2016) Is control through utilization a cost effective *Prosopis juliflora* management strategy? *J Environ Manag* 168:74–86
- Gebremedhin GH, Bereket H, Daniel B, Tesfaye B (2015) Effect of biochar on yield and yield components of wheat and post-harvest soil properties in Tigray Ethiopia. *J Fertil Pestic* 6(158):2
- Gokila B, Baskar K (2015) Characterization of *Prosopis juliflora* L. biochar and its influence of soil fertility on maize in alfisols. *Int J Plant Animal Env Sci* 5(1):123–127
- Reddy KR, Yaghoubi P, Yukselen-Aksoy Y (2015) Effects of biochar amendment on geotechnical properties of landfill cover soil. *Waste Manag Res*. <https://doi.org/10.1177/0734242X15580192>
- Sadasivam BY, Reddy KR (2015) Engineering properties of waste wood-derived biochars and biochar-amended soils. *Int J Geotech Eng* 9(5):521–535. <https://doi.org/10.1179/1939787915Y.0000000004>
- Yargicoglu EN, Sadasivam BY, Reddy KR, Spokas K (2015) Physical and chemical characterization of waste wood derived biochars. *Waste Manag* 36(2015):256–268
- Pardo GS, Sarmah AK, Orense RO (2017) Mechanism of improvement of biochar on shear strength and liquefaction resistance of sand. *Geotechnique* 69(6):471–480
- Kumar H, Ganesan SP, Bordoloi S, Sreedeeep S, Lin P, Mei G, Garg A, Sarmah AK (2019) Erodibility assessment of compacted biochar amended soil for geo-environmental applications. *Sci Total Environ* 672:698–707
- Garg A, Bordoloi S, Ni J, Cai W, Mddibiona PG, Mei G, Poulsen TG, Lin P (2019) Influence of biochar addition on gas permeability in unsaturated soil. *Geotech Lett*. <https://doi.org/10.1680/jgele.18.00190>
- Chen YZ, Zhou WH, Liu F, Yi S, Geng X (2019) Microstructure and morphological characterization of lead-contaminated clay with nanoscale zero-valent iron (nZVI) treatment. *Eng Geol* 256:84–92. <https://doi.org/10.1016/j.enggeo.2019.05.001>
- Zhou WH, Qi XH (2019) Root cohesion estimation of Riparian trees based on model uncertainty characterization. *J Mater Civ Eng* 31(2):04018389. [https://doi.org/10.1061/\(asce\)mt.1943-5533.0002600](https://doi.org/10.1061/(asce)mt.1943-5533.0002600)
- Chen YZ, Zhou WH, Liu F, Yi S (2019) Exploring the effects of nanoscale zero-valent iron (nZVI) on the mechanical properties of lead-contaminated clay. *Can Geotech J*. <https://doi.org/10.1139/cgj-2018-0387>
- Zhou WH, Liu F, Yi S, Chen YZ, Geng X, Zheng C (2018) Simultaneous stabilization of Pb and improvement of soil strength using nZVI. *Sci Total Environ* 651(Pt1):877–884. <https://doi.org/10.1016/j.scitotenv.2018.09.146>
- Zhou WH, Xu X, Garg A (2016) Measurement of unsaturated shear strength parameters of silty sand and its correlation with unconfined compressive strength. *Measurement* 93:351–358. <https://doi.org/10.1016/j.measurement.2016.07.049>
- Wong JTF, Chen ZK, Ng CWW, Wong MH (2015) Gas permeability of biochar-amended clay: potential alternative landfill final cover material. *Environ Sci Pollut Res* 23(8):7126–7131
- Jeffery S, Meinders MB, Stoof CR, Bezemer TM, van de Voorde TFJ, Mommer L, van Groenigen JW (2015) Biochar application does not improve the soil hydrological function of a sandy soil. *Geoderma* 251:47–54
- Ronsse F, Van Hecke S, Dickinson D, Prins W (2013) Production and characterization of slow pyrolysis biochar: influence of feedstock type and pyrolysis conditions. *GCB Bioenergy* 5(2):104–115
- Lee Y, Park J, Ryu C, Gang KS, Yang W, Park YK, Jung J, Hyun S (2013) Comparison of biochar properties from biomass residues produced by slow pyrolysis at 500 C. *Bioresour Technol* 148(2013):196–201
- Enders A, Lehmann J (2012) Comparison of wet-digestion and dry-ashing methods for total elemental analysis of biochar. *Commun Soil Sci Plant Anal* 43(7):1042–1052
- Pourakbar S, Asadi A, Huat BB, Fasihnikoutalab MH (2015) Stabilization of clayey soil using ultrafine palm oil fuel ash (POFA) and cement. *Transp Geotech* 3:24–35
- Gupta C, Sharma RK (2016) Black cotton soil modification by the application of waste materials. *Period Polytech Civ Eng* 60(4):479
- Gupta S, GuhaRay A, Kar A, Komaravolu VP (2018) Performance of alkali-activated binder-treated jute geotextile as reinforcement for subgrade stabilization. *Int J Geotech Eng*. <https://doi.org/10.1080/19386362.2018.1464272>
- Miao S, Shi J, Sun Y, Zhang P, Shen Z, Nian H, Zhang P (2018) Mineral abundances quantification to reveal the swelling property of the black cotton soil in Kenya. *Appl Clay Sci* 161:524–532
- Liu X, Han F, Zhang X (2012) Effect of biochar on soil aggregates in the loess plateau: results from incubation experiments. *Int J Agric Biol* 14(6):975–979
- Reddy KR, Yargicoglu EN, Yue D, Yaghoubi P (2014) Enhanced microbial methane oxidation in landfill cover soil amended with biochar. *J Geotech Geoenviron Eng* 140(9):04014047
- Garg A, Bordoloi S, Ni J, Cai W, Maddibiona PG, Mei G, Poulsen TG, Lin P (2019) Influence of biochar addition on gas permeability in unsaturated soil. *Geotech Lett* 9(1):66–71
- Bordoloi S, Garg A, Sreedeeep S, Lin P, Mei G (2018) Investigation of cracking and water availability of soil-biochar composite synthesized from invasive weed water hyacinth. *Bioresour Technol* 263:665–677
- Garg A, Hazra B, Zhu H, Wen Y (2019) A simplified probabilistic analysis of water content and wilting in soil vegetated with non-crop species. *CATENA* 175:123–131